Science Arena Publications
Specialty Journal of Engineering and Applied Science
ISSN: 2520-5943
Available online at www.sciarena.com
2018, Vol, 3 (1): 1-18

Determining Member Deflection of a Four-Bar Linkage based on Concentrated Masses Method

Mohsen Vesal
Mechanic and aerospace academic compound, Malek-e-Ashtar Industrial university
*Corresponding Author

Abstract: *The present study examined a simple four-bar mechanism. Four-bar linkage is one of the most common and most useful mechanisms in engineering. The first member of such a mechanism is ground to which the second and the fourth members are hinged and pivot about it. These two members are called cranks. The third member, the linking bar, is connected to two cranks. The members considered herein for the proposed mechanism are flexible which makes them have deflections during rotation. Each of the three integrated members of the proposed mechanism have been divided to discrete masses and their deflections have been computed for a given time period (from the beginning to the end of the motion). The more the members' divisions, the more realistic the answer to the problem will be. First of all, the mass point acceleration was calculated and then the motion equations of the members were obtained. Finally, the member deflection was computed using Euler-Bernoulli method.*

Keywords: *Elastic Four-Bar Mechanism, Concentrated Mass Method, Analytical and Numerical Solutions, Deflection*

INTRODUCTION

The elasticity theory in fact deals with the study of the extent to which the elastic environments undergo changes subject to stresses and exerted forces. Elasticity of an environment causes every deviant part to return to its initial equilibration. There are numerous studied conducted regarding elastic mechanisms. These researches have been focused on three mechanisms, namely basic four-bar linkage, slider-crank and rapid return.

Deformation in such mechanisms can be accompanied by unfavorable outcomes such as spatial imprecision, alternative stresses resulting in fatigue as well as unwanted vibration and noises. Moreover, instability of elastic mechanisms is of a great importance.

The entire dynamic analyses pertaining to the flexibility of the linkage members and robots are drawn on the member rigidity assumption which is of course not always true. It was deemed necessary with the progress in technology and fast increase in the machines' speed to reconsider the authenticity of the foresaid assumption because the system members' inertia forces effects are increased considerably in higher speeds that cause vibrations and elastic deformation at the same time with the system's rigid motion. The vast use of composite materials in machines added to the importance by twice as much of the studies in this regard.

It is evident considering the elastic deformations in such mechanisms that the input-output relationship differs from that of the rigid systems. Unlike the rigid state, the input-output relationship of the elastic mechanism cannot be solely obtained via mechanism geometry rather an elastodynamic analysis is required.

It is worth mentioning that attentions have been largely directed at flexibility of the mechanism hinges and robots plus the members' flexibility during the past few decades.

Many researches have been carried out on elastic mechanisms. Alexander and Lawrence experimentally investigated the dynamic response of the elastic mechanisms (Alexander R. M., et al., 1974; Alexander R. M., et al., 1973). They were the first who performed researches on the empirical analysis of perfectly elastic four-bar mechanisms. In (Winfrey R. C., 1971; Winfrey R. C., 1972; Erdman A. G., et al., 1972; Erdman A. G., et al., 1971; Imam I., et al., 1973) the elastic mechanisms were subjected to analytical studies. Sedler and Sonder investigated a four-bar mechanism based on concentrated mass method (Sadler J. P., et al., 1973). The model was based on nonlinear equations extracted according to Euler-Bernoulli theory. They obtained the elastic deformations of the three moving members of a four-bar mechanism. Sedler and Sonder calculated the dynamic strains and stresses of the four-bar mechanism members in another study (Sadler J. P., 1975). They also examined a four-bar mechanism only one member of which was elastic in another study (Sadler, J. p., et al., 1974). The present study deals with the analysis of an elastic four-bar mechanism based on concentrated mass method following which the Euler-Bernoulli theory will be used to compute the mechanism members' deformations.

Concentrated Mass Method and Equations Governing the Problem:

A member is divided to several equal parts in concentrated mass method and the total mass of every part is considered situated at the center. The volumetric mass of the entire body is assumed fixed hence the entire points have the same masses.

Figure (1) illustrates a bar featuring an elasticity module, E, and area moment of inertia, I. Considering a bar of the length L and dividing it to N equal parts, the length of each part will be equal to $2l = \frac{L}{N}$. If the mass of every part is considered positioned in the center, the total value of the point masses will be equal to the total mass of the bar.

$$M=\sum_{j=1}^{N} m_j \tag{1}$$

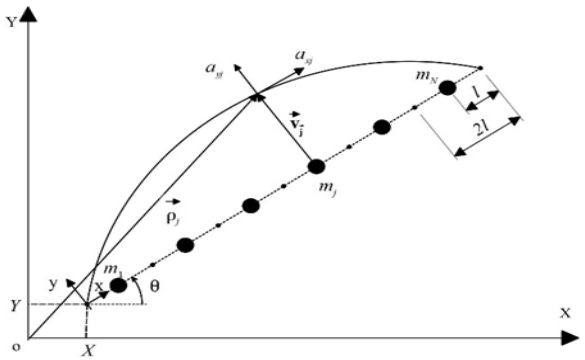

Figure 1. a double-hinged bar and its mass points

The planar motion of a rigid body is obtained by X(t) and Y(t) coordinates and θ(t) angle that are connected to X-Y coordinate system. The mobile x-y coordinate system is mounted on the beam and its deformation in respect to the beam axis is described by the function y (x, t). The boundary conditions for a double-hinged beam are as shown in equation (2).

$$y(0,t) = y(L,t) = 0 \tag{2}$$

The bend curve of the beam is expressed through the function $v_j(t)$, j=1, ..., N, where $v_j(t)$ is the transversal displacement of the mass m_j, (y (x, t) =vj(t)).

The position of the mass, mj, is expressed as demonstrated in equation (3) for a fixed coordinate along the mobile coordinate in which $\vec{\imath}$ and $\vec{\jmath}$ are the unit vectors.

$$\overrightarrow{\rho_j}=[X\cos\theta+Y\sin\theta+(2j-1)l]\,\vec{\imath}+[Y\cos\theta-X\sin\theta+v_j]\,\vec{\jmath} \quad (3)$$

Performing differentiation in respect to time twice on equation (3) gives the absolute acceleration of mj mass.

$$a_{xj}=\ddot{X}\cos\theta+\ddot{Y}\sin\theta-(2j-1)l\dot{\theta}^2-2\dot{\theta}\dot{v}_j-\ddot{\theta}v_j \quad (4)$$

$$a_{yj}=-\ddot{X}\cos\theta+\ddot{Y}\sin\theta+(2j-1)l\ddot{\theta}+\ddot{v}_j-\dot{\theta}^2v \quad (5)$$

the inertia of a member causes deflection in motion for which the D'Alembert's principle is used. The transversal and longitudinal forces pertinent to mj are: (Sadler J. P., et al., 1974)

$$D_{xj}=-m_ja_{xj} \quad (6)$$

$$D_{yj}=-m_ja_{yj} \quad (7)$$

These forces are the elastic members' forces and they can be also used when writing the external forces. According to figure (2), 01 is the beginning and A is the ending parts of the first arm; A is the beginning and B is the ending part of the second arm, as well. 02 is the beginning and B is the ending part of the third arm.

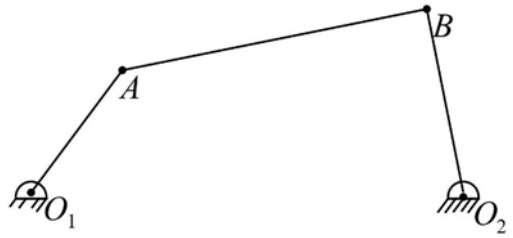

Figure 2. a four-bar mechanism featuring a hinge A between the first and the second members and the hinge B between the second and third members

It can be concluded based on figure (3) for all three arms using D'Alembert's principle and exerting the supporting forces on the first arm and writing the equilibrium equations that:

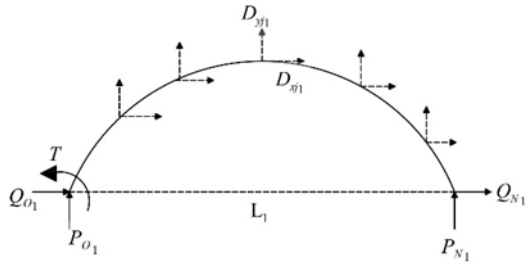

Figure 3. the free diagram of the first member of the four-bar mechanism

$$P_{o1}+P_{N1}\sum_{j=1}^{N_1}D_{yj1}=0 \quad (8)$$

$$P_{N1}.L1+\sum_{j=1}^{N_1}(2j-1)l_1D_{yj1}-\sum_{j=1}^{N_1}v_{j1}\,D_{xj1}+T=0 \quad (9)$$

Inserting equation (9) in equation (8) gives:

$$P_{N1} = -\sum_{j=1}^{N_1} \frac{l_1}{L_1}(2j-1)D_{yj1} + \sum_{j=1}^{N_1} \frac{v_{j1}}{L_1} D_{xj1} - \frac{T}{L_1} \quad (10)$$

$$P_{o1} = -\sum_{j=1}^{N_1} [\frac{l_1}{L_1}(2j-1) - 1]D_{yj1} - \sum_{j=1}^{N_1} \frac{v_{j1}}{L_1} D_{xj1} + \frac{T}{L_1} \quad (11)$$

As for the second and the third arm, it can be written similar to the first arm and without the torque T that:

$$+ \sum_{j=1}^{N_2} \frac{v_{j2}}{L_2} D_{xj2} \quad (12)$$

$$P_{o2} = -\sum_{j=1}^{N_2} \left[\frac{l_2}{L_2}(2j-1) - 1\right] D_{yj2} - \sum_{j=1}^{N_2} \frac{v_{j2}}{L_2} D_{xj2} \quad (13)$$

$$P_{N3} = -\sum_{j=1}^{N_3} \frac{l_3}{L_3}(2j-1)D_{yj3} + \sum_{j=1}^{N_3} \frac{v_{j3}}{L_3} D_{xj3} \quad (14)$$

$$P_{o3} = -\sum_{j=1}^{N_3} \left[\frac{l_3}{L_3}(2j-1) - 1\right] D_{yj3} - \sum_{j=1}^{N_3} \frac{v_{j3}}{L_1} D_{xj3} \quad (15)$$

Using the continuity equation for the hinge A, it can be written that:

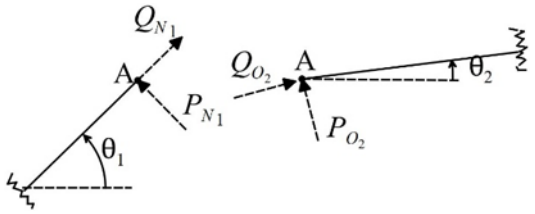

Figure 4. free diagram of the hinge A of the first and second members

$$P_{N1}\cos\theta_1 + Q_{N1}\sin\theta_1 + Q_{o2}\sin\theta_2 + P_{o2}\cos\theta_2 = 0 \quad (16)$$

$$P_{N1}\sin\theta_1 + P_{o2}\sin\theta_2 = Q_{N1}\cos\theta_1 + Q_{o2}\cos\theta_2 \quad (17)$$

The amounts of Q_{O2} and Q_{N1} are obtained in the form of equations (18) and (19) through solving the equations (16) and (17):

$$Q_{o2} = \frac{P_{N1} + P_{O2}\cos(\theta_1 - \theta_2)}{\sin(\theta_1 - \theta_2)} \quad (18)$$

$$Q_{N1} = \frac{P_{N1}\cos(\theta_2 - \theta_1) + P_{O2}}{\sin(\theta_2 - \theta_1)} \quad (19)$$

Using the continuity equation for the hinge B, it can be written that:

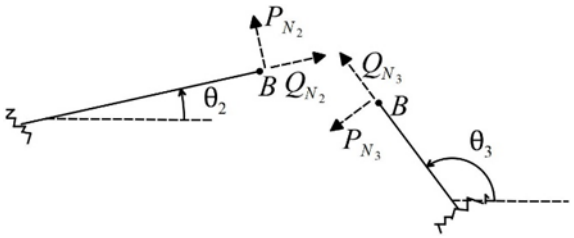

Figure 5. free diagram of the Hinge B of the second and third members

$$P_{N2}\cos\theta_2 + Q_{N2}\sin\theta_2 + P_{N3}\cos\theta_3 + Q_{N3}\sin\theta_3 = 0 \quad (20)$$

$$Q_{N2}\cos\theta_2 + Q_{N3}\cos\theta_3 = P_{N2}\sin\theta_2 + P_{N3}\sin\theta_3 \quad (21)$$

The amounts of Q_{O2} and Q_{N1} are obtained in the form of equations (22) and (23) through solving the equations (20) and (21):

$$Q_{N2}=\frac{P_{N3}+P_{N2}\cos(\theta_3-\theta_2)}{\cos(\theta_3-\theta_2)} \quad (22)$$

$$Q_{N3}=-\frac{P_{N3}\cos(\theta_3-\theta_2)+P_{N2}}{\sin(\theta_3-\theta_2)} \quad (23)$$

Having the Q_{N1}, Q_{N2} and Q_{N3} values, it can be concluded through writing the equilibrium equation along the first arm that:

$$Q_{o1}=-Q_{N1}-\sum_{j=1}^{N_1} D_{xj1} \quad (24)$$

Similarly, it can be concluded for the other two arms that:

$$Q_{o2}=-Q_{N2}-\sum_{j=1}^{N_2} D_{xj2} \quad (25)$$

$$Q_{o3}=-Q_{N3}-\sum_{j=1}^{N_3} D_{xj3} \quad (26)$$

The following measures are taken to calculate the force couple exerted on the first arm. Firstly, according to the relation (25) and inserting the relation (18) in lieu of Q_{O2}, it can be concluded that:

$$\frac{P_{N1}+P_{O2}\cos(\theta_1-\theta_2)}{\sin(\theta_1-\theta_2)}=-Q_{N2}-\sum_{j=1}^{N_2} D_{xj2} \quad (27)$$

Now, it can be written through inserting the relation (10) that:

$$\frac{-\sum_{j=1}^{N_1}\frac{l_1}{L_1}(2j-1)D_{yj1}+\sum_{j=1}^{N_1}\frac{v_{j1}}{L_1}D_{xj1}-\frac{T}{L_1}+P_{O2}\cos(\theta_1-\theta_2)}{\sin(\theta_1-\theta_2)}=-Q_{N2}-\sum_{j=1}^{N_2} D_{xj2} \quad (28)$$

Then, the amount of T couple is obtained in the form of equation (29) through organizing the abovementioned relation:

$$T=L_1\sin(\theta_1\theta_2)\left[\frac{-\sum_{j=1}^{N_1}\frac{l_1}{L_1}(2j-1)D_{yj1}+\sum_{j=1}^{N_1}\frac{v_{j1}}{L_1}D_{xj1}+P_{O2}\cos(\theta_1-\theta_2)}{\sin(\theta_1-\theta_2)}+Q_{N2}+\sum_{j=1}^{N_2} D_{xj2}\right] \quad (29)$$

The static equilibrium equations include 9 equilibrium equations and 4 continuity equations in A and B hinges.

Next, the deflection equations of all the mass points of the four-bar mechanism members are written. The deformation equation is obtained using Euler equation for elastic curve. The linear form of the Euler's differential equation for the beams is as shown in equation (30):

$$EI\frac{\partial^2 y}{\partial x^2}=M(x,t) \quad (30)$$

Where, M (x, t) is the flexural moment in point x. Assuming a trivial value of deflection allows the substitution of the approximate term $\frac{\partial^2 y}{\partial x^2}$ for elastic curvature but the assumption does not cancel the participation of the longitudinal forces in the transversal displacement of the beam. The finite difference approximation transforms the partial differential equation, shown in relation (30), to an ordinary equation system, relation (31).

$$EI\left(\frac{\Delta^2 v}{\Delta x^2}\right)_i=M_i(t) \quad (31)$$

Through expanding second-order Taylor polynomial for y_{i-1} and y_i around x_i point, we will have:

$$y_{i-1}\approx y_i-\Delta x_i(\frac{\partial y}{\partial x})_i+\frac{1}{2}(\Delta x_i)^2(\frac{\partial^2 y}{\partial x^2})_i \quad (32)$$

$$y_{i+1}\approx y_i+\Delta x_{i+1}(\frac{\partial y}{\partial x})_i+\frac{1}{2}(\Delta x_{i+1})2(\frac{\partial^2 y}{\partial x^2})_i \quad (33)$$

Omitting $(\frac{\partial y}{\partial x})_i$ from the above equation and considering $v_i=y_i$:

$$(\frac{\Delta^2 v}{\Delta x^2})_i=\frac{2}{\Delta x_i\Delta x_{i+1}(\Delta x_i+\Delta x_{i+1})}[\Delta x_{i+1}v_{i-1}-(\Delta x_i+\Delta x_{i+1})v_i+\Delta x_i v_{i+1}] \quad (34)$$

The exertion of equation (31) on various mass points on the beam results in motion equation. The motion equations for the first arm, second arm and third arm include N_1 equations, N_2 equations and N_3 equations, respectively:

$$i=1 \qquad \frac{EI}{8l^2}(-8v_1+\frac{8}{3}v_2)=M_1 \quad (35)$$

$$i=2,3,\ldots,N-1 \qquad \frac{EI}{8l^2}(2v_{i-1}-4v_i+2v_{i-1})=M_i \quad (36)$$

$$i=N \qquad \frac{EI}{8l^2}(\frac{8}{3}v_{N-1}-8v_N)=M_N \quad (37)$$

The bending moments, M_i, of the three members of the four-bar mechanism considering the members' cross-section are calculated as shown in the equations (38), (39) and (40):

$$M_{i1}=(2i-1)l_1P_{o1}-v_{i1}Q_{01}+\sum_{j=1}^{i}2(i-j)l_1D_{yj1}-\sum_{j=1}^{i}(v_{i1}-v_{j1})D_{xj1}-T \quad (38)$$

$$M_{i2}=(2i-1)l_2P_{o2}-v_{i2}Q_{02}+\sum_{j=1}^{i}2(i-j)l_2D_{yj2}-\sum_{j=1}^{i}(v_{i2}-v_{j2})D_{xj2} \quad (39)$$

$$M_{i3}=(2i-1)l_3P_{o3}-v_{i3}Q_{03}+\sum_{j=1}^{i}2(i-j)l_3D_{yj3}-\sum_{j=1}^{i}(v_{i3}-v_{j3})D_{xj3} \quad (40)$$

Analyzing the Position, Velocity and Angular Acceleration:

A planar four-bar mechanism has been displayed in figure (6). The 01 and 02 hinges are fixed parts of the mechanism and A and B hinges' deflections are zero. The A and B hinges' position is determined given the angular position of the first member. Therefore, the positions of the mechanism members are computed as below.

The closed loop condition of the mechanism is determined via the vector equation given in relation (41):

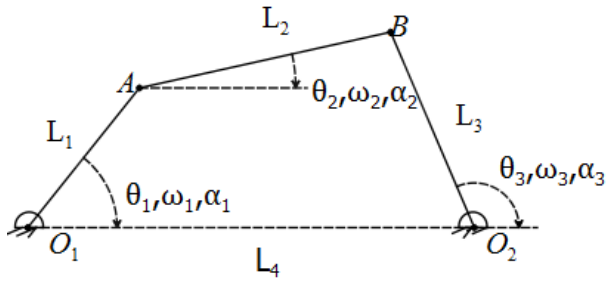

Figure 6. a planar four-bar mechanism with its first, second and third members featuring lengths equal to L_1, L_2 and L_3, respectively

$$L_1e^{i\theta 1}+L_2e^{i\theta 2}=L_4+L_3e^{i\theta 3} \quad (41)$$

Equation (42) is obtained through determining $L_2e^{i\theta 2}$:

$$L_2e^{i\theta 2}=L_4+ L_3e^{i\theta 3} -L_1e^{i\theta 1} \quad (42)$$

Equation (43) is obtained via considering the binary form of each sentence in equation (42):

$$L_2e^{-i\theta 2}=L_4+L_3e^{-i\theta 3}-L_1e^{-i\theta 1} \quad (43)$$

The multiplication sum of the equations (42) and (43) is given in equation (44):

$$L_2^2= L_4^2+ L_1^2+ L_3^2+ L_3 L_4(e^{i\theta 3}+e^{-i\theta 3})- L_1 L_4(e^{i\theta 1}+e^{-i\theta 1})-L_1L_3(e^{i\theta 1}. e^{-i\theta 3}+e^{-i\theta 1}. e^{i\theta 3}) \quad (44)$$

It can be concluded using Euler's expansion that:

$$L_2^2= L_4^2+ L_1^2+ L_3^2+ 2L_3 L_4\cos\theta_3- 2L_1 L_4\cos\theta_1- 2L_1 L_3 \cos\theta_3 \cos\theta_1- 2L_1 L_3 \sin\theta_3 \sin\theta_1 \quad (45)$$

It is written using trigonometric identities that:

$$\cos\theta_3=\frac{1-d^2}{1-d^2} \quad (46)$$

$$\sin\theta_3=\frac{2d}{1+d^2} \quad (47)$$

Where,

$$d=\tan(\frac{\theta_3}{2}) \quad (48)$$

Substituting these relations in equation (45) then multiplying them in $(1+d^2)$ and classification of the sentences gives:

$$ad^2+bd+c=0 \quad (49)$$

Where,

$$a= L_2^2- L_4^2- L_1^2- L_3^2+ 2L_3 L_4+2L_1 L_4\cos\theta_1- 2L_1 L_3\cos\theta_1$$

$$b=4L_1 L_3 \sin\theta_1$$

$$c= L_2^2- L_4^2- L_1^2- L_3^2+ 2L_3 L_4-2L_1 L_4\cos\theta_1+2L_1 L_3\cos\theta_1$$

$$d=\frac{-b\pm\sqrt{b^2-4ac}}{2a} \quad (50)$$

The two d values resulting from the equation gives two different θ3 values belonging to each branches of the mechanism. θ2 value is obtained using equations (51) and (52):

$$\text{Cos}\theta_2=\frac{L_4+L_3\cos\theta_3-L_1\cos\theta_1}{L_2} \quad (51)$$

$$\sin\theta_2=\frac{L_3\sin\theta_3-L_1\sin\theta_1}{L_2} \quad (52)$$

The velocity equation is obtained through differentiation using closed loop equation:

$$-L_1(\sin\theta_1)\ \omega_1-L_2(\sin\theta_2)\ \omega_2 +L_3(\sin\theta_3)\ \omega_3=0 \quad (53)$$

$$L_1\ (\cos\theta_1)\ \omega_1+L_2(\cos\theta_2)\ \omega_2-L_3(\cos\theta_3)\ \omega_3=0 \quad (54)$$

L1, L2, L3, L4 and θ1 are considered certain and θ2 and θ3 values are obtained from position analysis. Moreover, the angular velocity of the input link, slider, is definite. This way, the ungiven values of the above-cited equations are the angular velocities of the levers 2 and 3.
Therefore, these equations can be rewritten in the form of equations (55) and (56):

$$A\omega_2+B\,\omega_3=C \tag{55}$$
$$D\omega_2+E\,\omega_3=F \tag{56}$$

Where, the A to F values are calculated as demonstrated below:

$$A=-L_2\,(\sin\theta_2)$$
$$B=L_3\,(\sin\theta_3)$$
$$C=L_1\,(\sin\theta_1)$$
$$D=L_2\,(\cos\theta_2)$$
$$E=-L_3\,(\cos\theta_3)$$
$$F=-L_1\,(\cos\theta_1)\,\omega_1 \tag{57}$$

Such a writing style clearly indicates that equations (55) and (56) are linear considering such ungiven values as ω_2 and ω_3. Solving this pair of equation gives:

$$\omega_2=\frac{FB-EC}{DB-EA} \tag{58}$$
$$\omega_3=\frac{DC-FA}{DB-EA} \tag{59}$$

The acceleration equations are obtained through time-based differentiation of velocity equations:

$$-L_1(\cos\theta_1)\,\omega_1^2-L_1(\sin\theta_1)\,\alpha_1-L_2(\cos\theta_2)\,\omega_2^2-L_2(\sin\theta_2)\,\alpha_2+L_3(\cos\theta_3)\,\omega_3^2+L_3(\sin\theta_3)\,\alpha_3=0 \tag{60}$$

$$L_1(\sin\theta_1)\,\omega_1^2+L_1(\cos\theta_1)\,\alpha_1-L_2(\sin\theta_2)\,\omega_2^2+L_2(\cos\theta_2)\,\alpha_2+L_3(\sin\theta_3)\,\omega_3^2-L_3(\cos\theta_3)\,\alpha_3=0 \tag{61}$$

It is assumed in solving acceleration equation that θ1, ω1, α1, L1, L2, L3 and L4 are definite and that the θ2, θ3, ω2 and ω3 have been obtained from position and velocity analyses. Therefore, the only uncertainties of the abovementioned equations are the angular accelerations of links 2 and 3, to wit α2 and α3. So, the equations (60) and (61) can be rewritten as equations (62) and (63):

$$A\alpha_2+B\alpha_3=\acute{C} \tag{62}$$

$$D\alpha_2+E\alpha_3=\acute{F} \tag{63}$$

Where, A to F values are calculated as demonstrated in equation (64):

$$A=-L_2\,(\sin\theta_2)$$

$$B=L_3\,(\sin\theta_3)$$

$$C'=L_1(\cos\theta_1)\,\omega_1^2+L_1(\sin\theta_1)\,\alpha_1+L_2(\cos\theta_2)\,\omega_2^2-L_3(\sin\theta_3)\,\omega_3^2$$

$$D=L_2(\cos\theta_2)$$

$$E=-L_3(\cos\theta_3)$$

$$F'=L_1(\sin\theta_1)\,\omega_1^2-L_1(\cos\theta_1)\,\alpha_1+L_2(\sin\theta_2)\,\omega_2^2-L_3(\sin\theta_3)\,\omega_3^2 \tag{64}$$

A, B, D and E values are the same amounts used in velocity analysis hence there is no need for recalculating them. The forms of the equations (62) and (63) clearly show that they are linear in respect to such uncertainties as α2 and α3 and it can be concluded from solving them that:

$$\alpha_2=\frac{\acute{F}B-E\acute{C}}{DB-EA} \tag{65}$$

$$\alpha_3=\frac{D\acute{C}-\acute{F}A}{DB-EA} \tag{66}$$

Forming the Differential Equation System:

Equations (35), (36) and (37) pertain to the three arms, reaching in number to N1+N2+N3 equations, and they have to be solved together due to the fact that the reactions of the connections to the forces are coupled. To attain a set of systematic equations in regard of the aforementioned relations, M_i values have to be obtained from equations (38), (39) and (40) and the values of Po and Qo forces that had been previously obtained have to be replaced therein. It is in this case that the aforementioned equations will have D_{xi} and D_{yi} terms based on D'Alembert's forces. Finally, the equation system will be transformed into a second-order differential equation as shown in equation (67) by substituting equations (6) and (7).

$$[M]\{\ddot{v}\}+[k]\{v\}=\{F\} \tag{67}$$

The next stage is solving these equations through numerical integration. To calculate D_{xi} and D_{yi} terms, firstly $\ddot{X}$ and $\ddot{Y}$ values will be computed for all three arms. The first and the third members' hinges are immovable due to the fact that they are connected to a fixed point like the ground.

$$\ddot{X}_1=\ddot{Y}_1=0 \tag{68}$$

$$\ddot{X}_3=\ddot{Y}_3=0 \tag{69}$$

As for the second arm, the position equation of the hinge A is written. Then, it is differentiated twice based on time so that the $\ddot{X}$ and $\ddot{Y}$ pertaining to the second arm could be obtained.

$$X_2=L_1\cos\theta_1 \tag{70}$$

$$Y_2=L_1\sin\theta_1 \tag{71}$$

It can be written through twice integration of the relations (70) and (71) that:

$$\ddot{X}_2=-L_1(\ddot{\theta}_1\sin\theta_1+\dot{\theta}_1^2\cos\theta_1) \tag{72}$$

$$\ddot{Y}_2=-L_1(\ddot{\theta}_1\sin\theta_1+\dot{\theta}_1^2\cos\theta_1) \tag{73}$$

Values a_{xi} and a_{yi} will be obtained for all three arms through inserting $\ddot{X}$ and $\ddot{Y}$ values in relations (4) and (5) following the substitution of which in relations (6) and (7) D_{xi} and D_{yi} will be obtained for all three arms. Inserting the obtained values in relations (38), (39) and (40) and performing a little simplification provides for the omission of second-order values v and $v\ddot{v}$ due to their being trivial. Also, because the simplification operation is accompanied by the addition of a dampening matrix to equation (67) and it will be multiplied by the column vector $\{\dot{v}\}$, thus the amount $2\dot{v}\dot{\theta}$ is disregarded. In the end, values M_{i1}, M_{i2} and M_{i3} are calculated and inserted in equations (35), (36) and (37) that will be subsequently transformed to the equation system shown in relation (74):

$$[M]\{\ddot{v}\}+[k]\{v\}=\{F\} \tag{74}$$

Square Matrix [M] is the mass matrix and $(N_1+N_2+N_3)$-dimensional. The Matrix [K] is a square stiffness matrix featuring dimensions the same as mass matrix. The column vectors $\ddot{v}$, {v}, {F} and have $(N_1+N_2+N_3)$

members. The elements of the vector {v} respectively are the first, the second and the third members' mass point deflections. The general form of the mass and stiffness matrix is in such a way that the mass and stiffness equivalents of the first member's mass point, followed by those of the second member and then the third member are determined at first. Introducing an appropriate damping matrix [C] gives the equation (75) (Nath P. K., et al., 1980):

$$[M]\{\ddot{v}\}+[C]\{\dot{v}\}+[k]\{v\}=\{F\} \quad (75)$$

Matrix [c] can be considered as the linear combination of [M] and [K] matrices.

$$[C]=\beta_1[M]+\beta_2[K] \quad (76)$$

Where, β_1 and β_2 depend on the material from which the members are made.
The coefficients are functions of time in these equations. The solution method is as follows: the time domain is divided into several parts and it is assumed that the coefficients are constant for each of them. The method is advantageous in that the steady solution of each problem is obtained directly removing the need for long integrals in numerous consecutive cycles.

Numerical Solution of Differential Equations:

The equation (77) is a second-order ordinary differential equation which is nonlinear and coupled and it has to be solved numerically. The methods commonly used for numerical integration of such equations are: Rung-Kutta method, Wilson method and Newmark method. Herein, there was made use of Newmark method.

$$[M]\{\ddot{v}\}+[C]\{\dot{v}\}+[k]\{v\}=\{F\} \quad (77)$$

In Newmark method, the amounts of vectors $\{\ddot{v}\}$, $\{\dot{v}\}$ and $\{v\}$ for the instant t=tn are considered definite based on which the amounts of these same vectors are calculated for the instant $t= t_n+1$ and the determined amounts of these vectors for the foresaid instant are used for the next instant. The important point in such an operation is the solution stability and the lack of error accumulation. The solution is rendered stable considering an optimum value for Δt and proper amounts for α and β. Based on Newmark method, the differential equation system (77) is converted to the linear system of the equation (78):

$$[\bar{A}]\{v\}_{n+1}=\{P\}_{n+1} \quad (78)$$

Where, matrix $[\bar{\mathbf{A}}]$ and vector $\{P\}_{n+1}$ are transformed to equations (79) and (80):

$$[\bar{A}]=[K]+a_o[M]+a_5[C] \quad (79)$$

$$\{P\}_{n+1}=\{F\}_{n+1}+[n](a_o\{v\}_n+a_1\{\dot{v}\}_n+a_2\{\ddot{v}\}_n)+[C](a_5\{v\}_n+a_6\{\dot{v}\}_n+a_7\{\ddot{v}\}_n) \quad (80)$$

Where, the constant coefficients a_0 to a_7 are obtained as shown in relation (81):

$$a_o=\frac{1}{\beta\Delta t^2} \qquad a_1= ao\Delta t$$

$$a_2= \frac{1}{2\beta}-1 \qquad a_3=(1-\alpha)\Delta t$$

$$a_4=\alpha\Delta \qquad a_5=\frac{\alpha}{\beta\Delta t}$$

$$a_6=\frac{\alpha}{\beta}-1 \qquad a_7=\frac{\Delta t}{2}(\frac{\alpha}{\beta}-2) \quad (81)$$

The constant coefficients are found equal to $\alpha=\frac{1}{2}$ and $\beta=\frac{1}{4}$.

Solving the linear equation system gives the amount of the vector $\beta=\frac{1}{4}$ as demonstrated in the equation (82):

$$\{\ddot{v}\}_{n+1}= a_o(\{v\}_{n+1}-\{v\}_n) - a_1\{\dot{v}\}_n- a_2\{\ddot{v}\}_n \quad (82)$$

Therefore, the vector $\{\dot{v}\}_{n+1}$ is calculated as shown in the equation (83):

$$\{\dot{v}\}_{n+1}=\{\dot{v}\}_n+ a_3\{\ddot{v}\}_n+ a_4\{\ddot{v}\}_{n+1} \quad (83)$$

The amounts of $\{\ddot{v}\}_{n+2}$, $\{\dot{v}\}_{n+2}$ and $\{v\}_{n+2}$ can be obtained through rewriting the abovementioned equations and repeating this same process gives the amount of the vector and its temporal derivatives for any instant (J. N. Reddy, 2005).

The preliminary conditions for solving this differential equation are a $\{v\}_n$ vector value and its temporal derivatives at t=0. It is assumed in solving the equation that the amounts of all the vectors are zero in the onset, meaning that the motion begins from a static state and with no elastic deformation. There are four boundary conditions in solving the equation. The number of the boundary conditions depends on the number of hinges used in the mechanism. The elastic deformation of the hinges is considered equal to zero. The fist hinge wherein the first member is connected to the ground, is fixed and its elastic displacement along the longitudinal and transversal axes occurs in point zero on which the torque force, T, is exerted. The fourth hinge is also fixed and with no exertion of torque force. The second hinge as the connection point of the first and second members, and the third hinge, as the connection point of the second and third members, both are devoid of any elastic deformation and exertion of torque force.

Statement of Problem, Diagrams and Results Analysis

The following data are the inputs to the mechanism depicted in figure (7):

E=200Gpa	I=2× 10^{-10}m4	ρ=7800 $\frac{Kg}{m^3}$	
L_1=0.3m	L_2=0.8m	L_3=0.6m	L_4=0.7m
m_1=0.118kg	m_2=0.314kg	m_3=0.235kg	
n_1=5	n_2=13	n_3=10	θ_1=30°
T=3Sec	N=30	α_1=0.85$\frac{rad}{s^2}$	ω_1=0.1$\frac{rad}{s}$

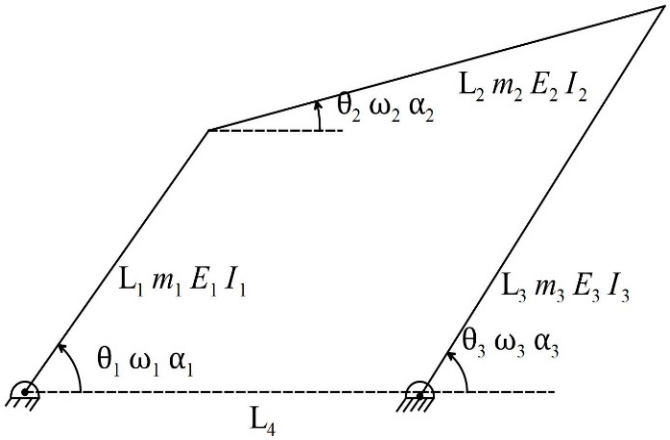

Figure 7. a four-bar mechanism and its variables

The mechanism members feature filled and uniform circular cross-sections and they are made of steel. In the computer program that has been written using MATLAB software, the θ_2, θ_3, ω_2, ω_3, α_2 and α_3 values are firstly obtained at the n-th instant after inserting the input data then the stiffness matrix [k] and mass matrix [M] are calculated. Next, θ_2, θ_3, ω_2, ω_3, α_2 and α_3 values are obtained at (n+1)-th instant based on which the force

matrix [F] amounts are calculated following which Newmark method is used to determine the elastic displacement values of all the masses. The motion is considered zero for all of the masses due to {v}, {v̇} and {v̈} being assumed zero.

Figure (8) exhibits the deflection diagram of the first and the third points of the first member for the given time span. It is evident from the diagram that the deflections of the two points are zero at the beginning of the motion and that the third point's deflection is higher than that of the first point for during the entire time span.

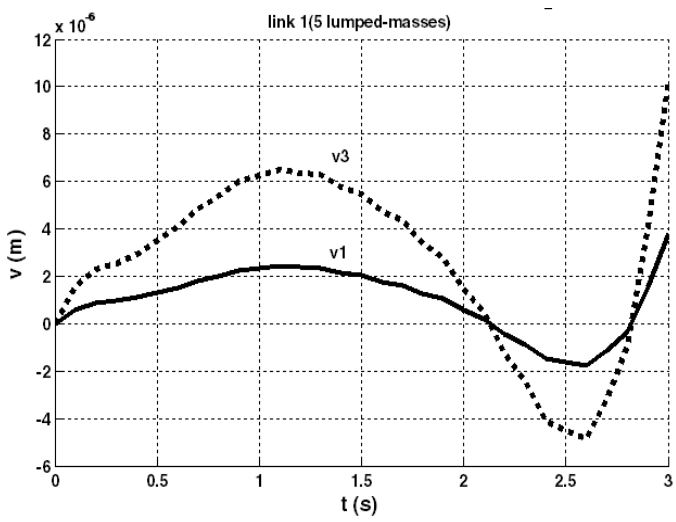

Figure 8. the deflection in the first member's first and third mass points in a four-bar mechanism in the course of time

Figure (9) illustrates the deflection diagram of the second and ninth mass points of the second member for a time span between zero and three second. As it can be seen, the mass points' deflection is opposite to the movement direction at the beginning of the motion. Also, the ninth mass point's deflection was found higher than that of the second mass point for the entire motion duration.

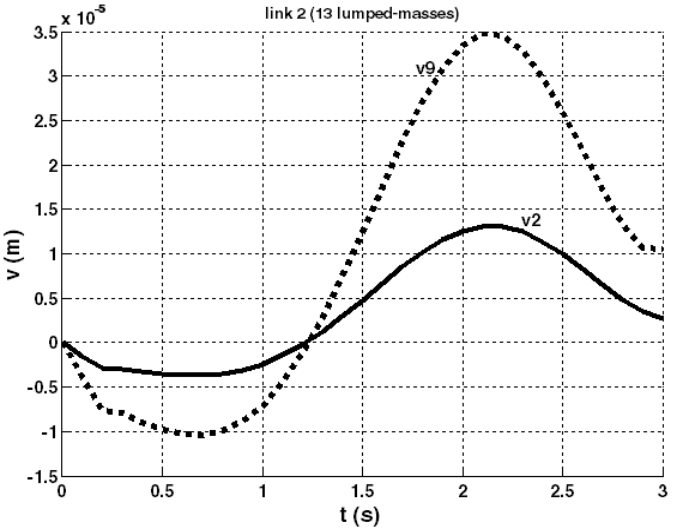

Figure 9. deflection in second and ninth mass points of the second member of the four-bar mechanism in time

Figure (10) demonstrates the deflections of the second and sixth mass points of the mechanism's third member. The deflections are opposite to the movement direction in the beginning of the motion. Moreover, the

sixth mass point is situated in the midsection of the third member and its deflection is always higher than the member's second mass point.

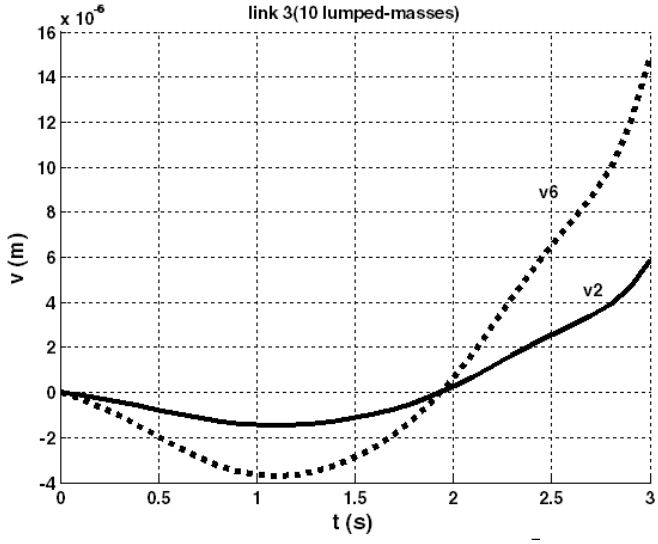

Figure 10. the deflections of the third member's second and sixth mass points in a four-bar mechanism in time

Figure (11) shows the deflection of the second member's mass points for two different mass divisions of the second member. As it can be observed, the deflections of the beginning and ending parts of the member are zero. Furthermore, it was found out that the middle points have deflections higher in rate than the lateral points. The two diagrams almost match for the two mass divisions indicating the authenticity of the results.

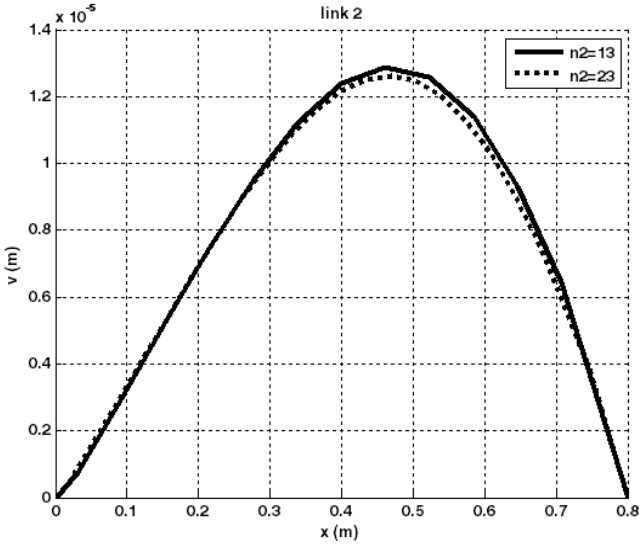

Figure 11. the deflection of the four-bar mechanism's second member based on the bar length for the two different mass divisions

Figure (12) displays the third member's deflection for two mass divisions in a given instant. It can be understood from the diagram that the beginning and the ending mass points of the third members have no deflections and the midpoints of the members have the highest deflection rates. The match of the two diagrams for these two different states is reflective of the accuracy of the results.

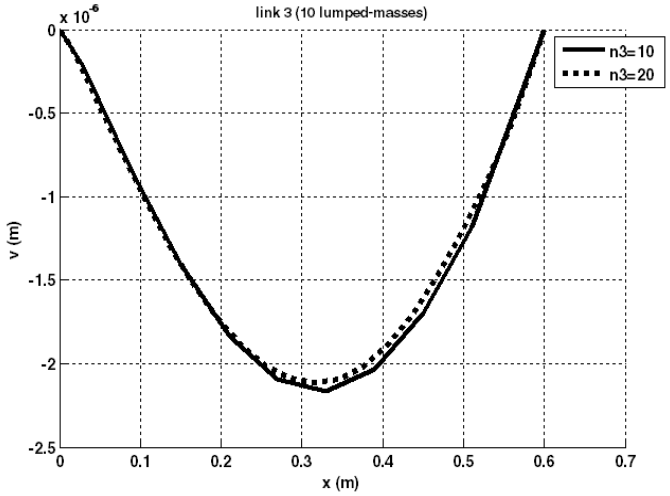

Figure 12. the deflection of the four-bar mechanism's third member in terms of the bar length for two different mass divisions

Figure (13) depicts the first mass point of the first member of the mechanism for two different temporal divisions. The diagram is expressive of the idea that the deflections of the point undergo direction shifts twice during the given time span. In addition, the two similar diagrams for two different states are assertive of the idea that the results are correct.

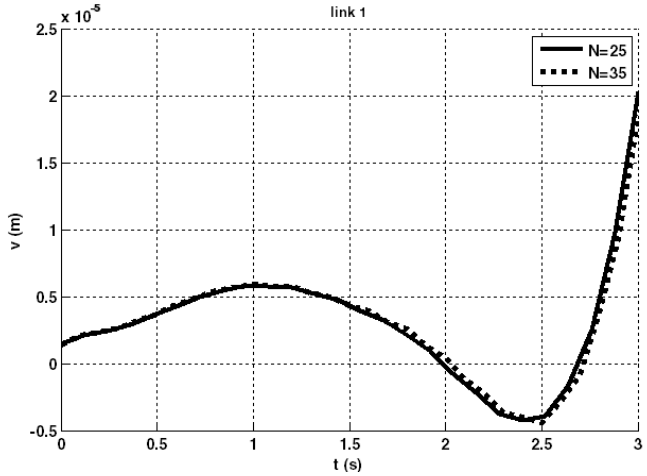

Figure 13. the deflection of the first mass point of the four-bar mechanism's first member for two states featuring different temporal divisions

Figure (14) illustrates the deflection of the mechanism's first member for a given instant. The diagram shows that the two extreme ends of the member have no deflections and the midsection mass point features the highest deflection.

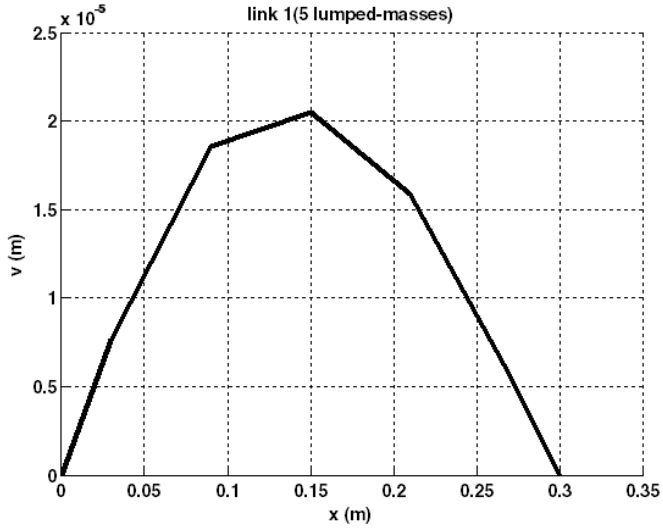

Figure 14. the deflection of the mass points of the four-bar mechanism's first member based on bar length

Figure (15) demonstrates the deflections of the second and the fourth mass points respectively for five and nine mass divisions for a fixed time span. The validity of the results is confirmed according to the fact that both these points are located in the middle part of the member for both of the states and both of the diagrams look similar.

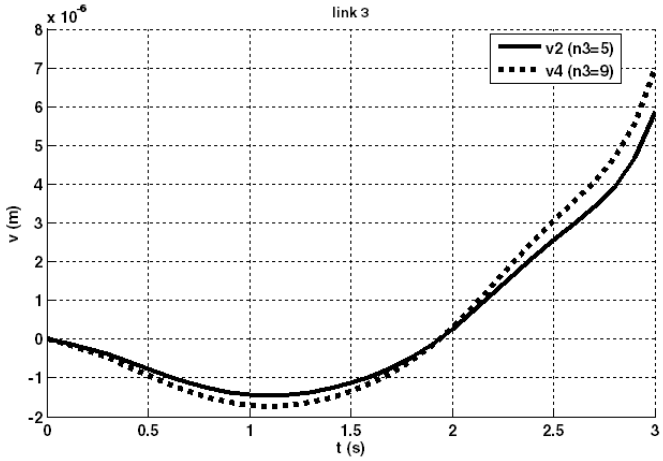

Figure 15. the deflections of the four-bar mechanism (midsection of bar)'s second and fourth mass points for various divisions based on bar length

Figure (16) depicts the deflection of the first member's second mass point for two different elasticity modules. The mass point deflection is lesser in a state the elasticity module of which is higher than the other.

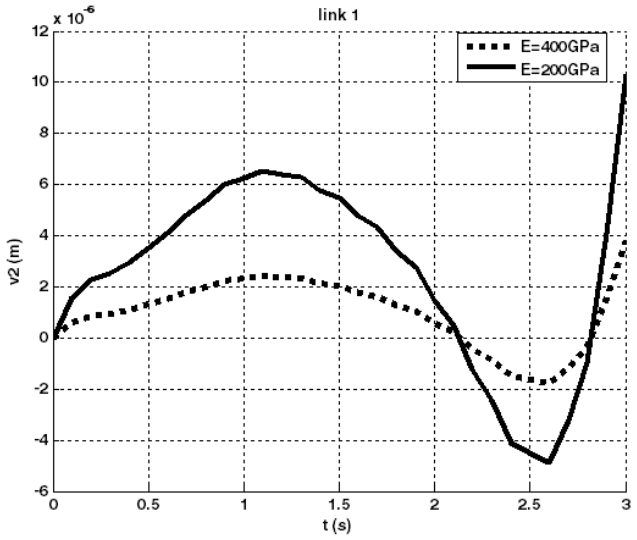

Figure 16. the deflection of the four-bar mechanism's second mass point for two different elasticity modules based on time

Figure (17) demonstrates the deflection of the second member's fourth point for two states featuring different cross-section diameters in time. The cross-section of the mass point is found reduced with the increase in the inertia moment and this is well complying with the reality so the results' credibility is affirmed.

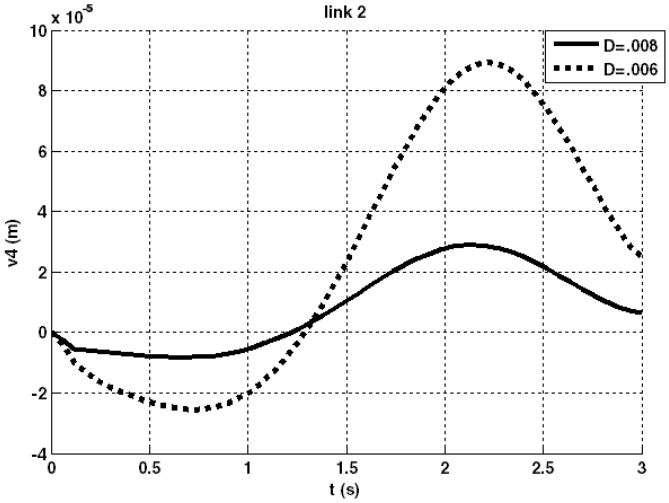

Figure 17. the deflection of the fourth mass point of the four-bar mechanism's second member for two different cross-sections in time

Figure (18) displays the elastic deformation of the tenth mass point of the mechanism's second member for two different states in different temporal divisions ranging from zero to three seconds. The two diagrams present better overlap with the increase in the number of the temporal divisions. As it can be seen, the two diagrams almost completely overlap one another and this underlines the accuracy of the results.

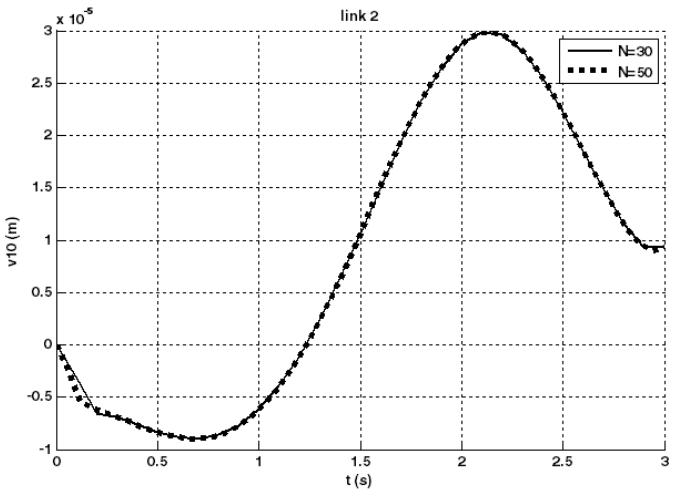

Figure 18. the deflection of the tenth mass point of the four-bar mechanism's second member for two different temporal divisions in a given time

Figure (19) exhibits the deflection of the mechanism's second member in a given time for two different temporal divisions. The diagrams were frequently found overlapping in the temporal divisions which is indicative of the accuracy of the results.

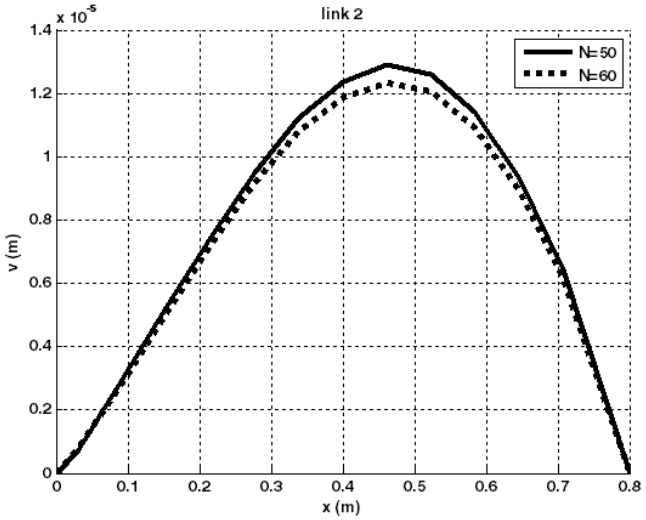

Figure 19. the deflection of the four-bar mechanism's second member for two different temporal divisions based on member's length

Results

To analyze a four-bar mechanism featuring elastic members, the present study firstly employed most widely used methods, including concentrated mass method and member deformation equations. Then, the member equilibrium equations were written to form a differential equation system assisted by the determination of mass points' acceleration. In the end, the differential equations' system was numerically solved and the deflections of the mechanism's members were attained.

In numerically solving differential equations using a computer program, the numerical method's error is significantly reduced if the number of the temporal divisions for a limited time span is increased to the extent that it can be stated that the responses will not undergo changes with the increase in the temporal divisions

and a series of precise responses can be obtained. Increasing the number of the mass divisions in concentrated mass method makes the responses approach the element model. To decrease the members' deflection, the area moment of inertia can be reduced or member featuring lower elasticity modules can be used to obtain more optimum conditions.

As for the numerical solutions of the differential equations, the mass points' velocity and acceleration, besides their deformations, are also computable considering the fact that there are also first and second derivatives extant in the equations.

Reference

1. Alexander, R. M., and Lawrence, K. L., "An Experimental Investigation of the Dynamic Response of an Elastic Mechanism," Journal of Engineering for Industry, Trans. Asme, Series B, Vol. 96, No. 1, Feb. 1974, pp. 268-274.
2. Alexander, R. M., and Lawrence, K. L., "Dynamic Strains in a Four Bar Mechanism," Proceedings of the Third Applied Mechanism Conference, Stillwater, Okla., 1973, Paper No. 26.
3. Erdman, A. G., Imam, I., and Sandor, G. N., "Applied Kineto-Elastodynamics," Proceedings of the Second Applied Mechanism Conference, Stillwater, Okla., 1971, Paper No. 21.
4. Erdman, A. G., Sandor, G. N., and Oakberg, R. G., "A General Method for Kineto-Elastodynamic Analysis and Synthesis of Mechanisms," Journal of Engineering for Industry, Trans. Asme Paper, 71-WA/DE-6.
5. Imam, I., Sandor, G. N., and Kramer, S. N., "Deflection and Stress Analysis in High Speed Planar Mechanisms with Elastic Links," Journal of Engineering for Industry, Trans. Asme, Series B, Vol. 95, No. 2, May 1973, pp. 541-548.
6. J. N. Reddy, An Introduction to The Finite Element Method, Third Edition, Mc. Graw. Hill, New York, 2005.
7. Nath, P. K., and Gosh, A., Kineto-Elasto Dynamic Analysis of Mechanisms by Finite Element Method, J. Machine Theory, vol 15, 1980, PP. 179-179.
8. Sadler, J. P., "On the Analytical Lumped-Mass Model of an Elastic Four-Bar Mechanism," Journal of Engineering for Industry, May 1975, pp. 561-565.
9. Sadler, J. p., and Sander, G. N., "Nonlinear Vibration Analysis of Elastic Four-Bar Linkages," Journal of Engineering for Industry, Trans. Asme, Series B, Vol. 96, No. 2, May 1974, pp. 411-419.
10. Sadler, J. P., and Sandor, G. N., "A lumped Parameter Approach to Vibration and Stress Analysis of Elastic Linkages," Journal of Engineering for Industry, Trans. Asme, Series B, Vol. 95, No. 2, May 1973, PP. 549-557.
11. Winfrey, R. C., "Dynamic Analysis of Elastic Link Mechanisms by Reduction of Coordinates," Journal of Engineering for Industry, Trans. Asme, Series B, Vol. 94, No. 2, May 1972, PP. 577-582.
12. Winfrey, R. C., "Elastic Link Mechanism Dynamics," Journal of Engineering for Industry, Trans. Asme, Series B, Vol. 93, No. 1, Feb. 1971, PP. 268-272.